PROPERTIES AND CRYSTALLIZATION OF PLLA BIOPOLYMERS WITH CELLULOSE NANOCRYSTALS AND ORGANIC PLASTICIZER

MARTIN BORUVKA, LUBOS BEHALEK, JAN NOVAK

Technical University of Liberec, Faculty of Mechanical Engineering, Czech Republic

DOI: 10.17973/MMSJ.2020_11_2020030

lubos.behalek@tul.cz

The paper deals with the research of ternary nanocomposites based on PLLA nucleated by lignin coated cellulose nanocrystals (L-CNC) and simultaneously modified with an acetyl tributyl citrate (ATBC) plasticizer. The potential synergistic effect of both additives on the crystallization and morphology of nanocomposites is evaluated by differential scanning calorimetry (DSC) and scanning electronic microscopy (SEM). Mechanical properties were evaluated by tensile tests and fracture toughness measurements. DSC analysis showed a synergistic effect of both additives on the crystallization of PLLA. Ternary composites which were plasticized by 10 mass% of ATBC and simultaneously nucleated by L-CNC (1 and 5 mass%) increased the degree of crystallinity up to 2.5 times and manage to eliminate undesired cold crystallization during reheating. A dramatic increase in ductility, associated with a decrease in tensile strength and modulus, was observed with the incorporation of ATBC at 10 mass%. The ductility of the PLLA/10ATBC and PLLA/10ATBC/1L-CNC composites increased from 3 % (PLLA) up to 160 % and 300 %, respectively. Furthermore, SEM analysis showed that higher concentrations of spray-dried L-CNC (5 mass%) are difficult to disperse by used technology. These agglomerates subsequently act as stress concentrators that initiate premature failure of the composites. Although a suitable combination of tensile characteristics was achieved, PLLA/10ATBC/1L-CNC composites still show relatively low Charpy impact strength (15 kJ/m^2).

KEYWORDS

Poly(lactic acid), cellulose nanocrystals, acetyl tributyl citrate

1 INTRODUCTION

At the beginning of the 21st century, the possibility of replacing petroleum-derived polymers with natural, abundant, and biodegradable materials was verified. The most promising bio-based, biodegradable, and biocompatible linear aliphatic polyester is poly (lactic acid) (PLA). PLA is industrially obtained by ring-opening polymerization of lactide at elevated temperatures and under the action of catalytic compounds. Lactide can be made through bacterial fermentation of lactic acid from renewable resources such as corn, cassava, or sugarcane. Due to the presence of central chiral carbon atom, there are two optical isomer forms of lactic acid: L-lactic and D-lactic acid. Therefore, during the production of PLA from lactide, three formations are possible: L-lactide made from two L-lactates (PLLA), D-lactide from two D-lactates (PDLA), and LD meso-lactide made from a combination of one L- and one D-lactate (PDLLA). Physical and mechanical properties are comparable to many conventional synthetic-based plastics. On the other hand, PLA also exhibits some properties that limit its use in technical applications, for example, low impact and heat resistance, slow crystallization rate, sensitivity to hydrolysis, and gas permeability [Zhao 2013]. Therefore, there are still many challenges for the full market acceptance in utilizing neat PLA as an engineering material. In the last few decades many strategies have been used to improve the property deficiency of PLA. To name some, strategies based on plasticization, copolymerization, and melt blending have been utilized [Ye 2013]. To extend PLA use in a high-performance application an increase in crystallinity is especially needed. The higher degree of crystallinity is a crucial parameter that improves PLA´s thermal resistance, mechanical and barrier properties [Tan 2016]. Therefore, many efforts by both academia and industry are focused on the improvement of PLA crystallization kinetics by addition of both heterogeneous nucleation agents to increase nucleation density and plasticizers to increase chain mobility [Saedlou 2012]. Several researchers improve PLA crystallization by various nucleating agents like talc [Yu 2012], barium sulfate ($BaSO_4$), titanium dioxide (TiO_2), calcium carbonate ($CaCO_3$) [Liao 2007], orotic acid (OA) [Qiu 2011] and cellulose nanocrystals (CNCs) [Vestena 2016]. Among those, CNC received significant interest of the scientific community due to its unique mechanical properties and biodegradability. Some research utilizes also various plasticizers and oligomers [Burgos 2013] to improve the ductility of PLA.

Therefore, the current work was dedicated to developing PLLA ternary systems based on both nucleating agent and plasticizer without sacrificing overall biodegradability. Hydrophobic spray-dried lignin coated CNC (L-CNC) were chosen as a biobased nucleating agents and acetyl tributyl citrate (ATBC) was chosen as a biobased plasticizer. The influence of potential synergistic effect of both additives on utility properties of PLLA based ternary systems were evaluated.

2 EXPERIMENTAL PROCEDURE

The commercial homopolymer Poly(L-lactic acid) Luminy L105, supplied by Total Corbition (Netherlands), was used for the experimental procedure. This material contains stereochemical purity ≥ 99 % (L-isomer), reaches absolute mass-average molecular mass 65 000 g/mol, melt flow index of 22 g/10min (ISO 1133-A), and melting point 175 °C (ISO 11357). Spray-dried lignin-coated cellulose nanocrystals (L-CNC) (BioPlus-L™ Crystals) with an average particle size of 4-5 nm in width and 50-500 nm in length (American Process Inc., USA) and acetyl tributyl citrate Citroflex A-4 (ATBC) in the form of an oil liquid (Vertellus Holdings LLC) were applied as nucleating agent and organic plasticizer.

2.1 Preparation of nanocomposites

The avoid hydrolytic degradation of PLLA during processing, both PLLA pellets, L-CNC powder, and ATBC (55 °C, 24 h.) were dried in a vacuum drying oven VD53 (Binder, Germany). The laboratory micro compounder MC 15 HT and micro injection moulding machine IM 12 (Xplore, Netherlands) were used as the primary processing devices. For compounding with parallel conical screws, a speed of 100 rpm and a constant temperature profile of 180 °C (within all temperature zones of the melting chamber) were used. The dispersion and distribution of the additives in the PLLA were ensured by a recirculation channel in the melting chamber of the microcomputer and were controlled by the level of the torque. The melt was extruded into the melting chamber of a micro-injection moulding machine and the axial movement of the piston injected the defined volume of the melt into the mould cavity in the next step. The mould cavity

complied with the shape of test specimens 1B (ISO 527). The temperature of the melting chamber was set at 190 °C, the injection pressure reached 0.5 MPa for 2 s and then was increased to 1.2 MPa for 20 s. The individual compositions of the prepared nanocomposite structures are listed in Table 1.

Table 1. Composition of nanocomposite structures

Sample code	Composition [mass%]		
	PLLA	ATBC	L-CNC
PLLA	100	-	-
PLLA/1 L-CNC	99	-	1
PLLA/5 L-CNC	95	-	5
PLLA/5 ATBC	95	5	-
PLLA/5 ATBC/1 L-CNC	94	5	1
PLLA/5 ATBC/5 L-CNC	90	5	5
PLLA/10 ATBC	90	10	-
PLLA/10 ATBC/1 L-CNC	89	10	1
PLLA/10 ATBC/5 L-CNC	85	10	5

2.2 *Differential scanning calorimetry analysis*

Differential scanning calorimetry (DSC) method on DSC 1/700 calorimeter (Mettler Toledo, Switzerland) according to ISO 11357 was used for the evaluation of thermal properties of nanocomposites and the effect of L-CNC and ATBC on PLLA crystallization. The instrument was calibrated via indium and zinc standard. About (10 ± 0.4) mg of sample was prepared from the cross-section of the test specimen on a rotating microtome Leica RM2255 (Leica Biosystem, Germany) for each formulation. These cuttings were put into an aluminum pan (about volume 40 μl), sealed, and then placed in the DSC chamber. An empty pan was used as a reference. The samples were heated from 0 to 200 °C, further than isothermal were kept for 180 s to remove previous thermal history and then cooled again. The second heating-cooling cycle analysis run at 10 °C/min heating/cooling ramp in a nitrogen atmosphere (flow rate 50 ml/min) to determine thermal transitions: primary melt crystallization temperatures and enthalpies (T_c, ΔH_c), glass transition temperature (T_g), cold crystallization temperatures and enthalpies (T_{cc}, ΔH_{cc}), pre-melt crystallization temperatures and enthalpies (T_{pc}, ΔH_{pc}), melting temperatures and enthalpies (T_m, ΔH_m). Further, the degree of crystallinity (X_C) was determined according to the Equation (1), where ΔH^0_m is the melting enthalpy of 100 % crystalline PLLA (106 J/g) [Sarasua, 1998] and w_m is the mass fraction of PLLA in the composites.

Table 2. Thermal analysis (DSC) data of PLLA and PLLA nanocomposites

Sample code	T_c [°C]	ΔH_c [J/g]	T_g [°C]	T_{cc} [°C]	ΔH_{cc} [J/g]	T_{pc} [°C]	ΔH_{pc} [J/g]	T_m [°C]	ΔH_m [J/g]	X_C [%]
PLLA	95.7	7.5	59.2	99.7	26.8	159.9	5.0	175.5	53.3	20.5
PLLA/1L-CNC	96.7	9.1	59.6	96.4	24.6	159.7	3.7	163.0	58.0	28.0
PLLA/5L-CNC	95.9	18.1	58.9	95.2	15.1	159.6	4.8	174.8	53.5	33.4
PLLA/5ATBC	89.4	19.6	48.0	91.0	10.1	153.9	6.0	173.6	52.7	36.3
PLLA/5ATBC/1L-CNC	93.1	20.8	50.8	88.1	10.4	152.1	4.5	173.5	54.4	39.6
PLLA/5ATBC/5L-CNC	92.4	24.3	47.6	91.1	8.8	152.9	3.8	172.9	52.7	42.0
PLLA/10ATBC	87.1	20.7	42.7	85.9	8.4	149.5	4.9	172.6	50.3	38.3
PLLA/10ATBC/1L-CNC	90.9	35.8	0	0	0	153.0	1.2	170.9	47.3	48.8
PLLA/10ATBC/5L-CNC	90.5	35.7	0	0	0	152.2	0.6	170.3	46.1	50.5

$$X_C = \frac{\Delta H_m - \Delta H_{pc} - \Delta H_{cc}}{\Delta H_m^0 \cdot w_m} \cdot 100 \ [\%] \quad (1)$$

2.3 *Morphology characterization*

The morphology of nanocomposite fractured surfaces was analyzed in a Carl Zeiss ULTRA Plus (Carl Zeiss, Germany) scanning electron microscope (SEM) with the ET-SE (Everhart-Thornley) detector at an acceleration voltage range of 2-5 kV. Unnotched samples were prepared from frozen (-50 °C, 12 h.) injection moulded tensile bars which were cryo-crushed on a Resil 5.5 (Ceast, Italy) testing machine. Fractured surfaces were platinum coated (thickness: 1 nm) with a sputter coater (Quorum Technologies Ltd, UK).

2.4 *Mechanical properties*

All mechanical properties were determined at ambient temperature (23 °C) on a total volume of 10 specimens for each performed test. The specimens after injection moulding had been stored in a climatic chamber by temperature 23 °C, relative humidity 50 % for 10 days before testing. Tensile strength (σ_m) and nominal tensile strain at break (ε_{tb}) were determined by method ISO 527/1B/50 and tensile modulus (E_t) by method ISO 527 /1B/1. Measurements were carried out on TiraTest 2300 (Labortech, Czech Republic) device with the axial extensometer 3542 (Epsilon Technology Co., USA). Unnotched samples (80 x 10 × 4 mm) for impact tests were prepared from injection moulded tensile bars. The Charpy impact strength was evaluated according to ISO 179–1/1eU (unnotched samples) on Resil 5.5 (Ceast, Italy) testing machine. A pendulum with the nominal energy of 5 J and 2.9 m/s striking velocity was used. Ten specimens were tested for each material.

3 RESULTS AND DISCUSSION

3.1 *Crystallization of PLLA nanocomposites*

The PLLA homopolymer (compared to the commonly available PLA) does not contain a minor content of D-lactide (1-5 mass%) and thus polymer matrix achieves a higher degree of crystallinity (Table 2).

The effect of the incorporation of 1 and 5 mass% L-CNC on the crystallization of pure and plasticized PLLA (with 5 and 10 mass% ATBC) is clear from Fig. 1. In binary unsoftened nanocomposites, an increase in exothermic conversion in areas of primary crystallization from the melt is observed which results in a higher degree of crystallinity of PLLA. Although L-CNC acts as nucleating agent, no significant shift in melt crystallization temperature (T_c) to higher values was observed (Fig. 1 and Table 2).

Conversely, with increasing ATBC content, the crystallization peak of PLLA broadens and shifts to lower temperatures. The increased chain mobility of macromolecules allows PLLA to crystallize even at lower temperatures. Due to the expansion of crystallization temperatures, the enthalpy of crystallization (ΔH_C) increases. The synergistic effect of L-CNC and ATBC on the

trends of PLLA crystallization can be observed in ternary nanocomposites. The incorporation of L-CNC shifts the crystallization temperatures (Tc) of plasticized PLLA back to higher values. The fact can be stated that the increasing volume of L-CNC induces an increase in enthalpy of crystallization (ΔH_C) in nanocomposites plasticized with 5 mass% of ATBC. For nanocomposites with 10 mass% of ATBC, there is no further increase in enthalpy of crystallization (ΔH_C) as the weight fraction of L-CNC increases (above 5 mass%). This behavior indicates that ternary nanocomposites fully crystallized during the cooling process, and the enthalpy of crystallization (~36 J/g) is the limit value they could reach at a given cooling rate.

From the DSC curves in the heating phase (Fig. 2) the trend is visible, that with a decreasing amount of ATBC in the PLLA, a decrease in the glass transition temperature (T_g), and enthalpy associated with recrystallization and melting of the PLLA (ΔH_{pc} and ΔH_m). This decrease is due to an increase in intermolecular distance (reduction of intermolecular forces) and an increase in the mobility of macromolecular chains. Changes of enthalpy values in cold crystallization area (ΔH_{cc}) are inversely proportional to changes of enthalpy values in the melt crystallization area (ΔH_c). As the ability of PLLA to crystallize from the melt increases, the volume crystalizing under cold conditions decreases. With the addition of L-CNC (increasing the primary crystallization of the material), it is possible to observe a decrease in cold crystallization (ΔH_{cc}) and a shift of its temperature (T_{cc}) to lower values (Fig. 2). Similarly, with the increasing proportion of ATBC, the values of cold crystallization enthalpy (ΔH_{cc}) decrease and its temperature (T_{cc}) shifts to lower values due to the increased mobility of PLLA macromolecules.

In the case of ternary composites, the synergistic effect of both additives can be observed, especially in the case of nanocomposites with 10 mass% ATBC. Due to the synergistic effect of both additives, the crystallization was fully completed already during the cooling phase, and the material thus did not show a visible glass transition or cold crystallization during heating. The movement of macromolecules in the amorphous region was thus limited by the crystalline regions of PLLA. As Arrieta et al. [Arrieta 2015] stated, by increasing the degree of crystallinity of PLA, its barrier properties can be increased as well. This synergistic effect of ATBC and L-CNC can contribute to a wider application potential of PLA, e.g. in the packaging industry in the replacement of synthetic polymers.

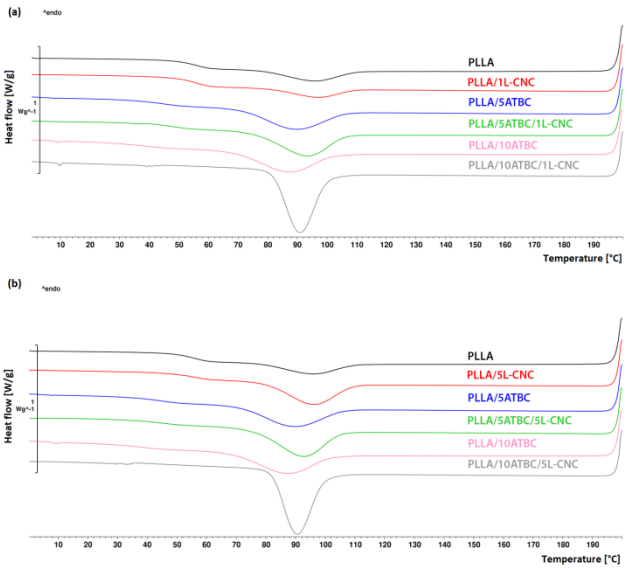

Figure 1: DSC curves of PLLA polymers with cellulose nanocrystals and acetyl tributyl citrate at cooling rate 10 °C/min

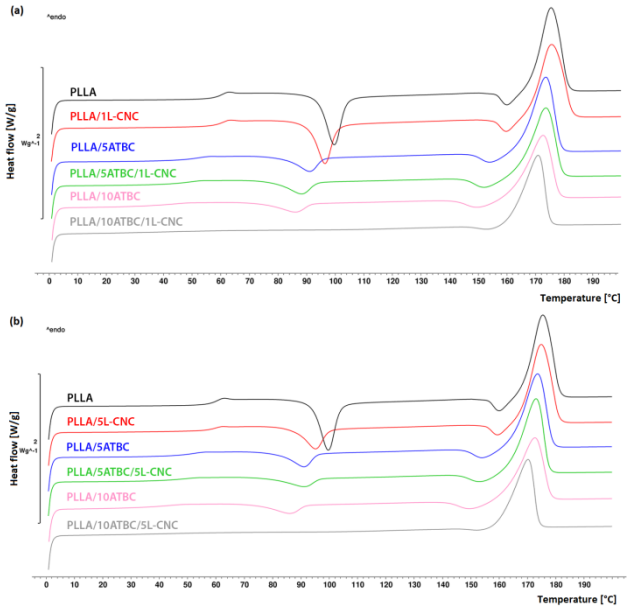

Figure 2. DSC curves of PLLA polymers with cellulose nanocrystals and acetyl tributyl citrate at heating rate 10 °C/min

3.2 Morphology characterization

PLLA exhibits the brittle type of failure typical for amorphous polymers. Fig. 3a shows a smooth surface with a laminated fracture structure. A similar type of failure can be observed for nanocomposites with 1 mass% L-CNC (Fig. 3b). Agglomerated cellulose nanocrystals with a size of about 10 µm are visible within the fracture surface. Nanocomposites with 5 mass% L-CNC also performed a brittle fracture, but the surface morphology shows a coarser structure. This type of failure indicates multiple crack propagation due to L-CNC agglomerates. Thus, it can be stated that during the preparation of PLLA / L-CNC nanocomposites the dispersion of cellulose nanocrystals in the PLLA melt is the key problem. PLLA fracture surfaces with 5 mass% ATBC and 1 and 5 mass% L-CNC also showed brittle fracture (Fig. 4). Although the addition of ATBC increases the spacing among the chains of macromolecules and increases their mobility, this aspect alone cannot generally prevent the fragility of PLLA. Low molecular weight ATBC is unable to absorb impact energy in a direction perpendicular to the orientation of macromolecules. The brittle failure occurs due to the high strain rate and low initiation energy for the formation of fragments and microcracks in the brittle PLLA.

L-CNC agglomerates are also visible in ternary composites (Fig. 4). Neither the addition of ATBC nor the prolongation of the dispersion phase in the preparation process had a positive effect on the individualization of L-CNC in the PLLA matrix.

The PLLA / 10ATBC and PLLA / 10ATBC / 1L-CNC (5L-CNC) composites again performed brittle fractures (Fig. 5). However, PLLA / 10ATBC / 1L-CNC ternary composites did not show L-CNC agglomerates within the fracture surface (Fig. 5b). This fact indicates a good individualization, dispersion, and distribution of cellulose nanocrystals during the preparation (compounding) of nanocomposites.

From the SEM images, the result can be stated, that the addition of ATBC cannot be visually identified in the fracture area. With poor compatibility, ATBC would be phase-separated and would be observed in the form of small spherical structures on the surface of the fracture, as described by Ren et al. in their study [Ren 2006]. ATBC reaches good solubility and miscibility in PLLA due to polar interactions between the ester groups of PLLA and the plasticizer. All plasticized PLLA samples showed signs of small

plastic deformations in the form of deformed protuberated fibrils.

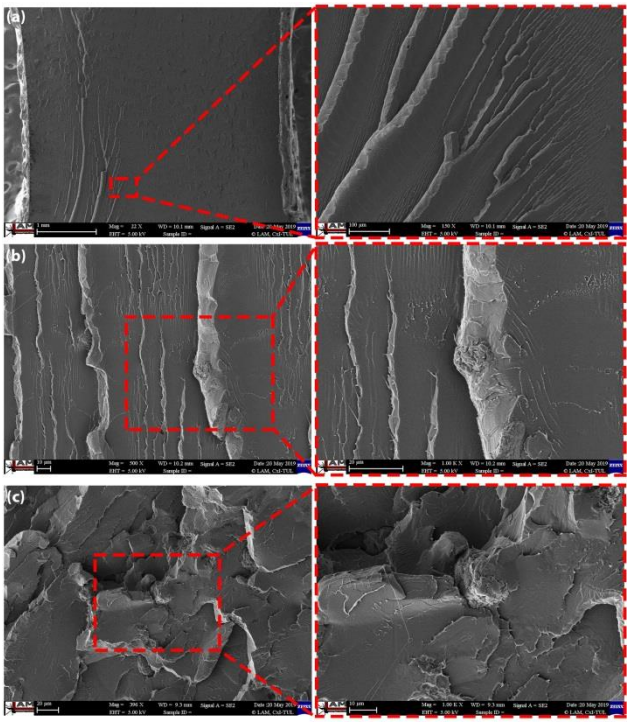

Figure 3. SEM images of fracture surfaces: (a) PLLA, (b) PLLA/1L-CNC, (c) PLA/5L-CNC

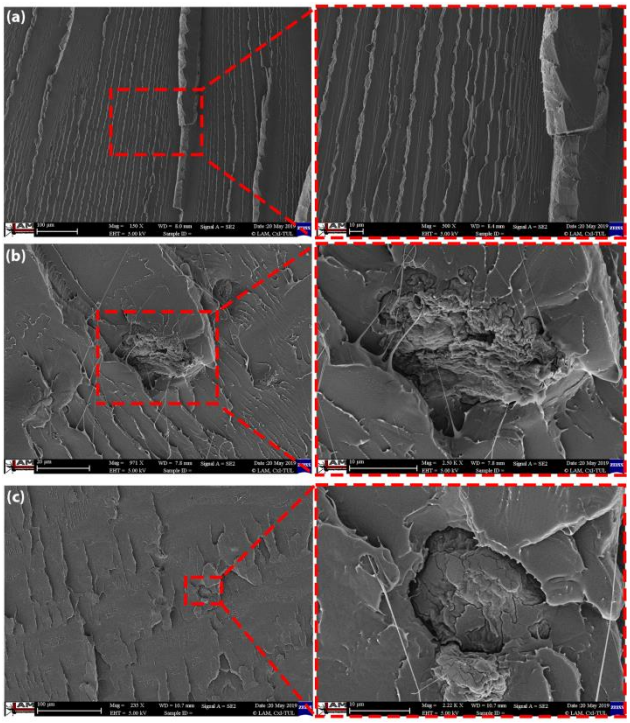

Figure 4. SEM images of fracture surfaces: (a) PLLA/5ATBC, (b) PLLA/5ATBC/1L-CNC, (c) PLA/5ATBC/5L-CNC

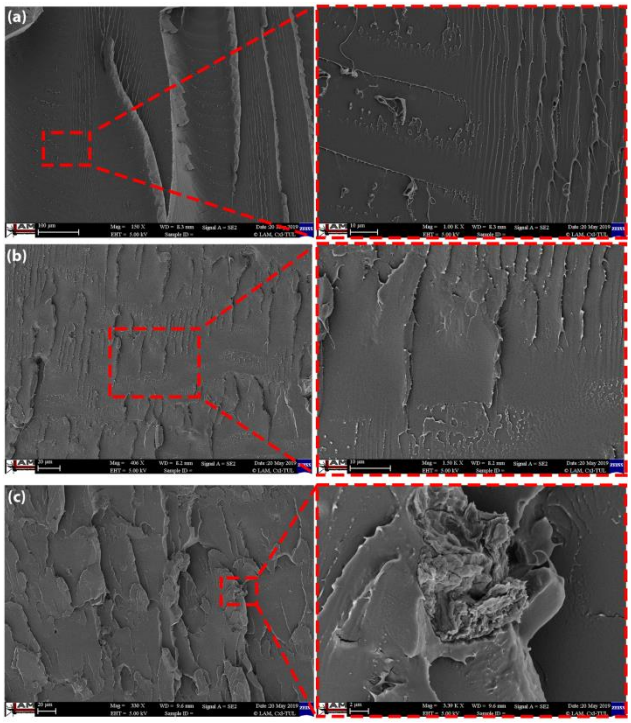

Figure 5. SEM images of fracture surfaces: (a) PLLA/10ATBC, (b) PLLA/10ATBC/1L-CNC, (c) PLA/10ATBC/5L-CNC

3.3 Mechanical properties

PLLA exhibits the typical behavior of a brittle amorphous thermoplastic with a relatively high tensile strength (σ_m), tensile modulus (E_t), and low nominal tensile strain (ε_{tb}). There was recorded no significant change in the mechanical properties of PLLA for binary nanocomposites with the addition of L-CNC. The decrease in the strength of PLLA / 5L-CNC is due to the higher occurrence of L-CNC agglomerates in the fracture surface (Fig. 3c). Samples with low ATBC content (5 mass%) did not reach the expected increase in ductility and also the tensile strength was reduced. Similar to binary nanocomposites, ternary nanocomposites with 5 mass% L-CNC showed the highest decrease in strength. There was no significant decrease in the values of the modulus of elasticity. With the incorporation of 10 mass% of ATBC, PLLA showed a significant decrease in strength and modulus of elasticity, accompanied by a significant increase in ductility. This finding corresponds to the results published by Cougneau [Courgneau 2011], who stated that a significant change in the modulus of elasticity occurs in PLA only with the incorporation of 9 mass% of ATBC. The values in Table 3 and the example in Fig. 6 show that with the addition of ATBC the PLLA deforms with a good possibility of orienting the chains of macromolecules in the direction of the tensile force. The deformation was accompanied by inhomogeneous plastic deformation and stress cracks (corresponding to the behavior of semicrystalline plastics with a lower degree of crystallinity). In ternary nanocomposites with 1 mass% of L-CNC, a decrease in the ability of macromolecular chains to orient with respect to the applied force was observed in the area of inhomogeneous plastic deformation with increasing elongation (the tensile strength of the material increases). This mechanism corresponds to the orientation of the lamellar structure in the direction of the applied force in semicrystalline polymers. This is the impact of the good dispersion, distribution, and individualization of the cellulose nanocrystals (Fig. 5b), which simultaneously in combination with ATBC led to an acceleration of the crystallization and to an increase in the degree of crystallinity of the PLLA. This synergistic effect of both additives led to an

increase in strength and ductility over plasticized PLLA / 10ATBC (Table 3). Table 3 further shows that this increase in ductility of the plasticized PLLA and ternary nanocomposites completely disappeared with the addition of 5 mass% L-CNC. This is due to premature failure of the material caused by higher amounts of solid particles in the form of agglomerates of cellulose nanocrystals, which failed to successfully disrupt during processing.

Table 3. Tensile properties of PLLA and PLLA nanocomposites

Sample code	σ_m [MPa]	E_t [MPa]	ε_{tb} [%]
PLLA	61.2 ±2.1	3422 ±15	3.2 ±0.3
PLLA/1L-CNC	60.8 ±2.7	3380 ±41	3.5 ±0.5
PLLA/5L-CNC	56.3 ±3.2	3509 ±55	2.9 ±0.2
PLLA/5ATBC	53.4 ±0.7	3332 ±98	2.8 ±0.7
PLLA/5ATBC/1L-CNC	53.0 ±1.2	3210 ±19	5.4 ±2.1
PLLA/5ATBC/5L-CNC	49.3 ±1.4	3290 ±52	3.7 ±0.4
PLLA/10ATBC	35.3 ±3.1	2620 ±114	158.2 ±14.5
PLLA/10ATBC/1L-CNC	42.2 ±2.9	2791 ±84	302.4 ±21.3
PLLA/10ATBC/5L-CNC	38.1 ±1.1	2805 ±53	4.6 ±1.8

When comparing PLLA with binary nanocomposites of PLLA based on L-CNC, the fact is obvious that a higher concentration of cellulose nanocrystals (5 mass%) led to a decrease in impact strength which is caused again by L-CNC agglomerates. Although the stiffness of cellulose nanocrystals is theoretically higher than that of steel, their density is many times lower and in the case of good dispersion, they can effectively absorb impact energy in the PLLA matrix.

In plasticized PLLA, a slight increase in impact strength was observed with increasing ATBC concentration. Murariu et al. states in his study [Murariu 2008] that the higher impact strength of PLA is manifested only at the ATBC content of 20 mass%. For ternary nanocomposites, a decrease in impact strength can be observed with a higher concentration of L-CNC (5 mass%). The impact strength values of these composites do not change depending on the amount of ATBC, and the decrease in impact strength is thus due to L-CNC agglomerates in the PLLA matrix, which initiate premature failure of nanocomposites. In contrast, for samples with 1 mass% L-CNC, the impact strength increases with increasing ATBC concentration (due to the uniform dispersion of cellulose nanoparticles).

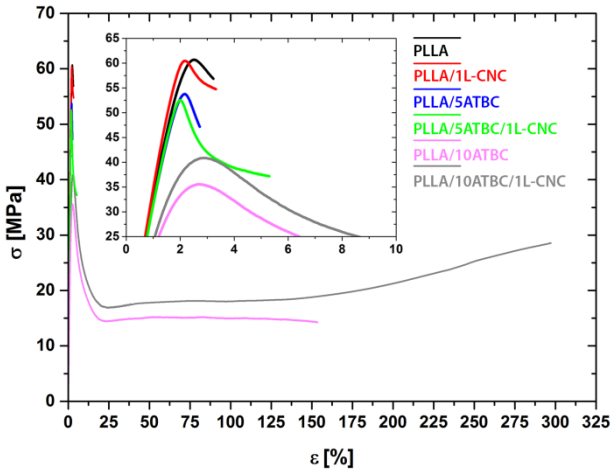

Figure 6. Tensile stress-strain curve of PLLA and PLLA nanocomposites

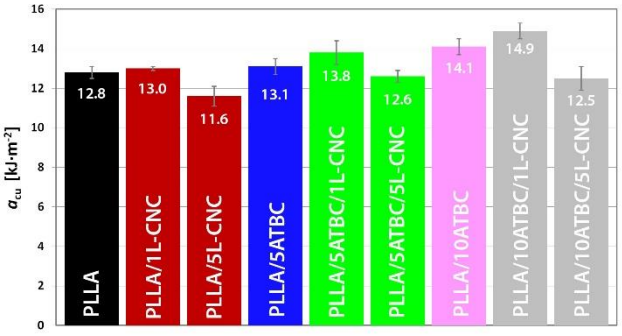

Figure 7. Charpy impact strength of PLLA and PLLA nanocomposites

4 CONCLUSIONS

In the preparation of PLLA nanocomposites based on L-CNC and ATBC, the dispersion of the agglomerated cellulose nanocrystals from their spray-dried form is the essential aspect. This was successfully reached with the PLLA / 10ATBC / 1L-CNC nanocomposite. DSC analysis showed a synergistic plasticized effect of both additives on the trend of crystallization and the resulting degree of crystallinity. The ternary composites PLLA / 10ATBC / 1L-CNC and PLLA / 10ATBC / 5L-CNC managed to increase the degree of crystallinity up to 2.5 times (at a cooling rate of 10 °C/min) and to eliminate undesired cold crystallization during reheating of the material.

Incorporation of ATBC at a lower concentration than 5 mass% did not have the desired effect on the mechanical properties of ternary nanocomposites. A dramatic increase in ductility, associated with a decrease in tensile strength and modulus of elasticity, was observed with the incorporation of 10 mass% ATBC. The ductility of the PLLA / 10ATBC and PLLA / 10ATBC / 1L-CNC composites increased from ~ 3 % (PLLA) to ~ 160 %, respectively ~ 300 %. The synergistic effect of well-dispersed nanocrystals of cellulose (1 mass%) and ATBC (10 mass%) in PLLA led to mechanical properties that are comparable to synthetic polymers such as PP, ABS or PBT. Although a suitable combination of tensile characteristics was achieved ($\sigma_m \cong 42$ MPa, $E \cong 2800$ MPa and $\varepsilon_{tb} \cong 300$ %), these systems still show low Charpy impact strength (~ 15 kJ/m^2).

This study also showed that higher concentrations of L-CNC (5 mass%) are difficult to disperse with the used technology and undisturbed agglomerates subsequently act as stress concentrators that initiate premature failure of the composites. The potential use of these materials can be found as the replacement of traditional materials in packaging technology. Their advantage is their natural origin, biodegradability and independence from fossil resources.

ACKNOWLEDGEMENT

This work was supported by the Student Grant Competition of the Technical University of Liberec under the project No. SGS-2019-5015 "Research and development for innovation of materials and production technologies with application potential in mechanical engineering“ and the EU - ESIF in the frames of Operational Programme Research, Development and Education - *project Hybrid Materials for Hierarchical Structures* (HyHi, Reg. No. CZ.02.1.01/0.0/0.0/16_019/0000843).

REFERENCES

[Arrieta 2015] Arrieta, M.P., at al. Bionanocomposite films based on plasticized PLA–PHB/cellulose nanocrystal blends. Carbohyd Polym, 2015, Vol. 121, pp. 265–275. ISSN 0144-8617

[Burgos 2013] Burgos, N., et al. Characterization and ageing study of poly(lactic acid) films plasticized with oligomeric lactic acid. Polym Degrad Stab, 2013, Vol. 98, pp. 651–658. ISSN 0141-3910
[Courgneau 2011] Courgneau, C., et al. Analysis of the structure-properties relationships of different multiphase systems based on plasticized poly (lactic acid). J Polym Environ, 2011, Vol. 19, No. 2, pp. 362–371. ISSN 1566-2543
[Liao 2007] Liao, R., et al. Isothermal cold crystallization kinetics of polylactide/nucleating agents. J Appl Polym Sci, 2007, Vol. 104, pp. 310–317. ISSN 1097-4628
[Murariu 2008] Murariu, M., et al. Polylactide (PLA) designed with desired end-use properties: 1. PLA compositions with low molecular weight ester-like plasticizers and related performances. Polymer Adv Tech, 2008, Vol. 19, No. 6, pp. 636–646. ISSN 1042-7147
[Qui 2011] Qiu, Z., et al. Effect of orotic acid on the crystallization kinetics and morphology of biodegradable poly (L-lactide) as an efficient nucleating agent. Ind Eng Chem Res, 2011, Vol. 50, pp. 12299–12303. ISSN 1520-5045
[Ren 2006] Ren, Z., et al. Dynamic mechanical and thermal properties of plasticized poly (lactic acid). J Appl Polym Sci, 2006, Vol. 101, No. 3, pp. 1583–1590. ISSN 1097-4628
[Saeidlou 2012] Saidlou, S., et al. Poly(lactic acid) crystallization. Prog Polym Sci, 2012, Vol. 37, pp. 1657–1677. ISSN 0079-6700
[Sarasua 1998] Sarasua, J.R., et al. Crystallization and melting behavior of polylactides. Macromolecules, 1998, Vol. 31, No. 12, pp. 3895–3905. ISSN 0024-9297
[Tan 2016] Tan, BH., at al. Recent progress in using stereocomplexation for enhancement of thermal and mechanical property of polylactide. ACS Sustain Chem Eng, 2016, Vol. 4, pp. 5370–5391. ISSN: 2168-0485
[Vestena 2016] Vestena, M., et al. Nanocomposite of poly (lactic acid)/cellulose nanocrystals: effect of CNC content on the polymer crystallization kinetics. J Braz Chem Soc, 2016, Vol. 27, pp. 905–911. ISSN 1678-4790
[Ye 2013] Ye, S., at al. Rubber toughening of poly(lactic acid): effect of stereocomplex formation at the rubber-matrix interface. J Appl Polym Sci, 2013, Vol. 128, pp. 2541–2547. ISSN 1097-4628
[Yu 2012] Yu, D., et al. Effects of talc on the mechanical and thermal properties of polylactide. J Appl Polym Sci, 2012, Vol. 125, pp. E99–E109. ISSN 1097-4628
[Zhao 2013] Zhao, H., Morphology and properties of injection molded solid and microcellular polylactic acid/polyhydroxy-butyrate-valerate (PLA/PHBV) blends. Ind Eng Chem Res, 2013, Vol. 52, pp. 2569–2581. ISSN 1520-5045

CONTACTS

Ing. Lubos Behalek, Ph.D.
Technical University of Liberec, Faculty of Mechanical Engineering, Department of Engineering Technology,
Studentska 1402/2, Liberec 1, 461 17, Czech Republic,
+420 48 535 3331, lubos.behalek@tul.cz, www.tul.cz